Tribol Lett (2010) 38:259–266
DOI 10.1007/s11249-010-9602-8

ORIGINAL PAPER

The Film Behaviors of Grease in Point Contact During Microoscillation

Gang Li · Chenhui Zhang · Hongyi Xu · Jianbin Luo · Shuhai Liu

Received: 4 December 2009 / Accepted: 30 March 2010 / Published online: 20 April 2010

Abstract Microoscillation is a typical case of transient motion, which occurs in many machine elements, including rolling or sliding element bearings, cams, and gears. Wear is easy to occur on the surface of such elements, particularly at the end point of the stroke, where the surfaces are momentarily static. In the present work, an experimental investigation is conducted to explore the grease film behavior of point contact lubrication during microoscillation in the case of pure rolling or pure sliding. The technique of relative optical interference intensity was used to monitor the variation of the grease film thickness and the motion of the grease in the contact area through analyzing the captured interferograms. Experimental results indicate that a crescent-shaped grease film can form along the motion direction in the contact area under microoscillation. The grease film is formed in the inlet region, and the film thickness remains while moving in the Hertzian contact area. In the case of pure rolling, the crescent-shaped grease film and the initial entrapped grease film are carried by a tow effect of moving interfaces in the contact area. However, in the case of pure sliding, there are relative motions in the sliding direction at the two interfaces of the grease/ball and the grease/disk in the Hertzian contact area. The shape of the entrapped grease remains almost unchanged while moving in the Hertzian contact area. During the repetition of microoscillations, the crescent-shaped grease film thickness drops gradually.

G. Li · C. Zhang (✉) · H. Xu · J. Luo · S. Liu
State Key Laboratory of Tribology, Tsinghua University, Beijing 100084, China
e-mail: chzhang@tsinghua.edu.cn

G. Li
e-mail: ligang06@mails.tsinghua.edu.cn

Keywords Grease · Film behavior · Microoscillation · Relative motion

1 Introduction

The majority of rolling or sliding element bearings, cams, and gears in use today are grease lubricated. However, grease is a complex multi-phase material as compared with Newtonian liquid lubricants. The effects of temperature, speed, and pressure on grease film thickness are well known, but the related mechanisms are not well understood [1, 2]. Many experimental investigations on grease have shown that the film behaviors depend on base oil viscosity, soap type and concentration, and most importantly, inlet lubricant supply [3–6]. However, most of these understandings of grease lubrication are restricted to steady-state conditions.

In practical cases, many moving-elements are working under transient conditions. Glovnea and Spikes [7] measured oil film thickness during reversal of entrainment in cyclically accelerated/decelerated motion, and the comparison of experimental results with an existing theoretical model showed that the measured minimum film thickness at the side of the contact was higher than the calculated value. Sugimura [8] suggested that the elastohydrodynamic film thicknesses under transient conditions deviated from those under steady-state conditions. Glovnea [9] found that when a sudden entrainment speed step was applied, the film thickness showed damped oscillations for about 30 ms before stabilizing at the steady-state value.

Taking into consideration that many grease lubricated moving-elements operate in oscillatory or intermittent fashion, the microoscillation can occur (the amplitude is close to the diameter of the Hertzian contact area) due to

the presence of inertia. In this case, moving-elements may suffer from fretting wear [10]. Kaneta et al. [11, 12] mentioned that a decrease in amplitude influenced oil film collapse, and then led to wear. McColl's work [13] indicated that the grease lubricant was capable of providing an effective shield around the fretting interface but was easily squeezed out of the main contact area. Zhou et al. [14] suggested that the ratio of the displacement amplitude to the radius of the Hertzian contact area was the most important parameter to affect the coefficient of friction using grease lubricant. These investigations are only concerned with the condition of the film formation under oscillation and the performance of the grease under fretting conditions.

Microoscillation is a typical case of transient motion. The entrainment velocity is always changing, and the amplitude of the microoscillation is very small, so the speed has to be very low. The newly formed lubricant film cannot flood the entire contact area. The theory of elasto-hydrodynamic lubrication could not apply to the case under microoscillation; therefore, it is essential to examine the behaviors of grease under microoscillation. The aim of the present study is to provide the basic characteristics of the grease film behaviors in the point contact area during reciprocating microoscillation through direct observations of the grease film using the technique of relative optical interference intensity.

2 Experimental Conditions

The technique of relative optical interference intensity was used to study the film formation and motion of the grease lubricant under microoscillation. The technique was originally developed for measuring thin fluid lubricant film thickness and profiles [15–17] and can be extended to measure the film thickness of grease under the oscillation condition [18]. A schematic diagram of the experimental measurement system and microoscillation is shown in Fig. 1, where L is amplitude, which represents the moving distance of the contact area, and D represents the diameter of the Hertzian contact area. In tests, in order to observe the behaviors of grease film in the contact area, the amplitude of the microoscillation was less than the diameter of the Hertzian contact area.

The contacting pairs are composed of a precision 7/8 inch diameter steel ball (Young's modulus $E = 210$ GPa and Poisson's ratio $v = 0.3$) and a glass disk ($E = 77.6$ GPa and $v = 0.17$) with a diameter of 180 mm and a thickness of 15 mm. The ball is loaded against the underside of the disk which is coated with a semi-reflecting chromium layer. The active surface roughness values (R_a) of the balls and the disk are about 5 and 2 nm, respectively.

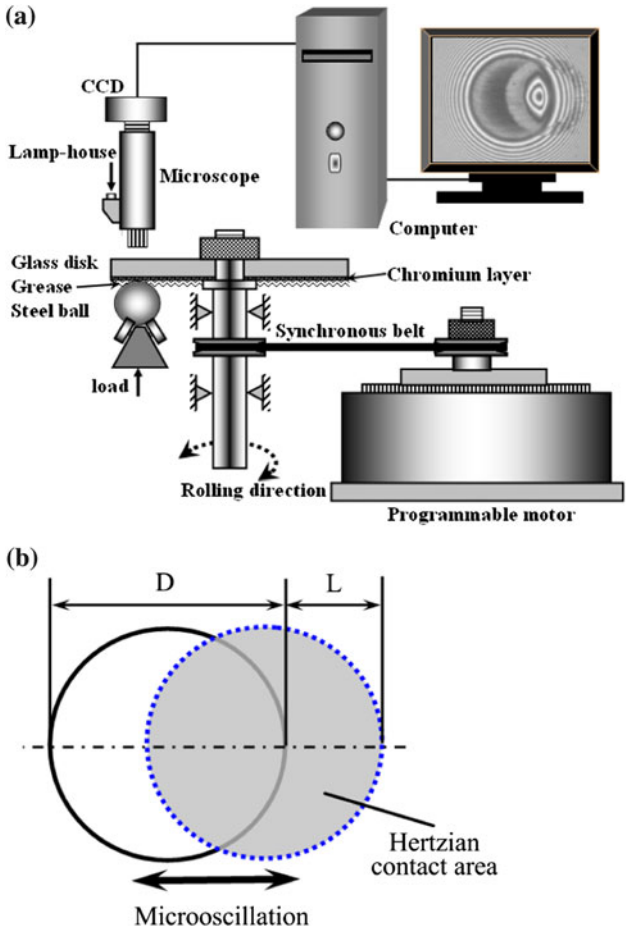

Fig. 1 Schematic diagram of the experimental apparatus and the microoscillation: **a** Schematic diagram of the experimental apparatus. **b** Schematic diagram of the microoscillation

The tests were conducted under rolling and sliding microoscillation conditions. In the case of the rolling microoscillation condition, the glass disk was driven by the programmable motor through a synchronous belt, and the steel ball was driven by the traction force transmitted through the contact point. For the sliding microoscillation condition, the steel ball was fixed, and pure sliding between the contact surfaces occurred. The controllable speed range of the programmable motor is from 0.0001 to 3 rev/s, and the acceleration/deceleration range is from 0.01 to 1280 rev/s^2. The disk rotation angle per step of the programmable motor is 0.01 degree.

The lithium grease was used as the lubricant in the tests, and its properties are listed in Table 1. The refractive index of the test grease is 1.435. All the tests were conducted at a temperature 25 ± 1 °C. Under the rolling condition, the ball and the disk were loaded together with an applied load of 22 N, which corresponded to a maximum Hertzian pressure of 0.497 GPa and a contact diameter of 0.292 mm. While under the sliding condition, the load was

Table 1 Physical parameters of the grease lubricant in the test

Soap type	Base oil viscosity (cSt)	Penetration unworked	Penetration worked	Dropping point (°C)
Lithium	150	280	280	180

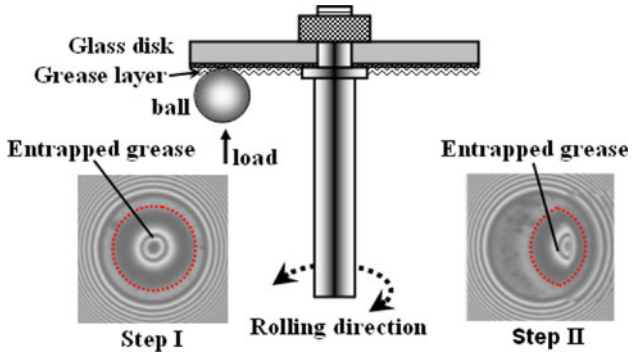

Fig. 2 The steps of the tests

14 N, providing a maximum Hertzian pressure of 0.423 GPa and a contact diameter of 0.252 mm. The tests were conducted at constant acceleration/deceleration of 0.44 m/s^2. The relationship between the maximum oscillation velocity and the oscillation amplitude can be expressed as:

$$V_{\max} = \sqrt{aL} \tag{1}$$

where $V_{\max}$ is the maximum oscillation velocity, a is the acceleration, and L is the oscillation amplitude.

As shown in Fig. 2, the tests were performed in two steps [19]. In the first step, the ball impacted the grease layer on the surface of the disk. As the two surfaces approached, the grease in the range of contact area cannot move out of the contact area in time, and some grease entrapped in the contact area [20–22]. The entrapped grease was marked by broken line in the central contact area. In the second step, the glass disk was driven by the motor in microoscillation. Before tests, the disk, the ball, and all the relevant parts of the apparatus were thoroughly cleaned with acetone and isopropanol in an ultrasonic bath.

3 Experimental Results

3.1 Behaviors of Grease Film During One Cycle Under the Rolling Microoscillation

The formation and distribution of the grease film in the central contact area can be seen from the set of interferograms in Fig. 3, and the two arrows indicate the motion directions. The zero entrainment positions occurred just at the instants of 0 T and 1/2 T in one cycle. Figure 3a–f

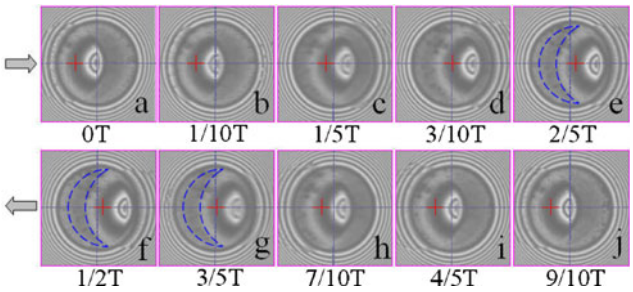

Fig. 3 Interferograms during one cycle under the rolling microoscillation (load is 22 N, amplitude is 0.122 mm)

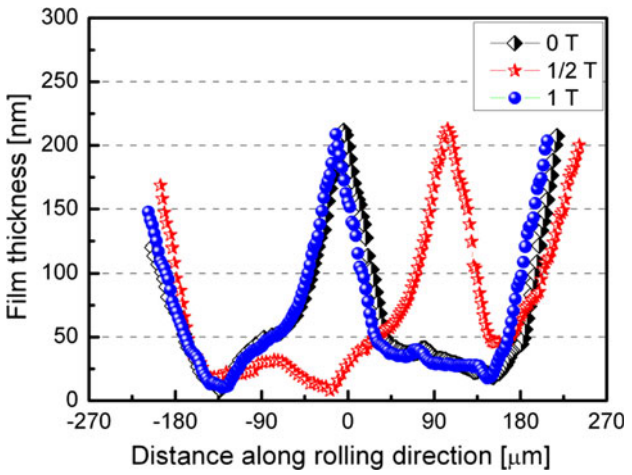

Fig. 4 The film thickness profiles along the rolling direction at the instants of 0, 1/2, and 1 T

corresponds to the first half period and the others correspond to the other half period. During the first half period, the entrainment inlet is on the left side of the contact area. It can be seen that the entrapped grease is carried by a tow effect of the moving surfaces to the outlet. The shape of the entrapped grease remains almost unchanged before it reaches the outlet zone. In addition, the new grease film moves into the contact area. Then, a crescent-shaped grease film occurs. Such a phenomenon was also observed by Kaneta et al. [23]. After reversal, the initial inlet becomes the outlet. The entrapped grease and the crescent-shaped grease film are carried by the tow effect of moving surfaces to the new outlet which can be seen from Fig. 3f–j. The shapes of the entrapped grease and the newly formed grease film remain almost unchanged before they arrive at the outlet edge, and the new grease film formed in the new inlet region.

Figure 4 shows the film profiles along the rolling direction at zero entrainment velocity instants (i.e., the instants of 0, 1/2, and 1 T). As can be seen, the film thickness profile of the entrapped grease remains almost unchanged when it moves in the contact area along the

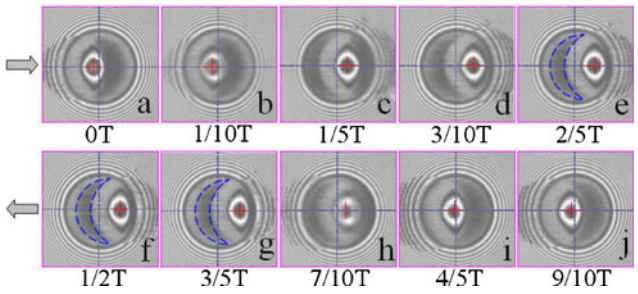

Fig. 5 Interferograms during one cycle under the sliding microoscillation (load is 14 N, sliding amplitude is 0.176 mm)

rolling direction, and the maximum film thicknesses of the entrapped grease does not change obviously in one cycle.

3.2 Behavior of Grease Film During One Cycle Under the Sliding Microoscillation

When the ball was kept fixed and the disk was driven by the motor, a series of interferograms were taken and given in Fig. 5, and the corresponding film thickness profiles along the sliding direction at the zero entrainment velocity in one cycle are shown in Fig. 6. The crescent-shaped grease film occurs gradually from the inlet, very similar to that find in the cases under the rolling conditions. However, a remarkable phenomenon appears. Under the sliding microoscillation, there are relative displacements in the sliding direction at the working interface between the ball and the glass disk in the contact area. As shown in Fig. 5, the entrapped grease is carried by the moving surface from the inlet side to the outlet side, and the shape of the entrapped grease remains almost unchanged before it moves out of the contact area. Because the steel ball is fixed, the position of the entrapped grease on the ball in the contact area is always changing. It can be deduced that relative motion occurs possibly near the grease/ball interface.

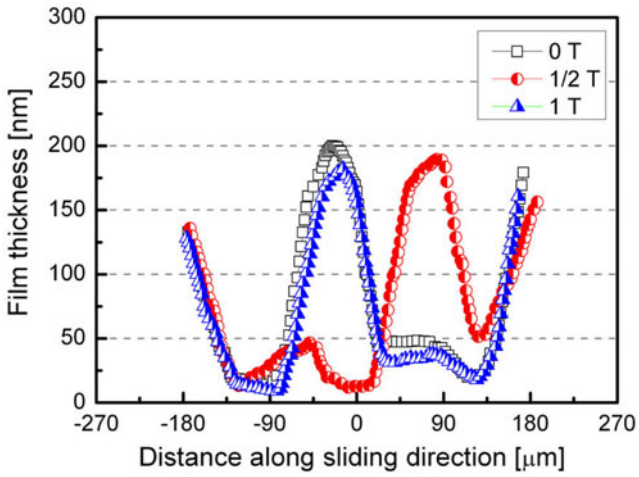

Fig. 6 The film thickness profiles along the sliding direction at the instants of 0, 1/2, and 1 T

As can be seen from Fig. 6, the film thickness profile of the entrapped grease remains almost unchanged when it moves in the contact area along the sliding direction, and the maximum film thicknesses of the entrapped grease decreases slightly in one cycle.

4 Discussion

4.1 Occurrence of Relative Motion in Central Contact Area

Under the sliding microoscillation condition, relative motion has been observed at the grease/ball interface. However, it cannot be confirmed that whether relative motion occurs near the grease/disk interface. In order to investigate the relative motion between the glass disk and the entrapped grease, a reference line was scratched on the working surface of the glass disk. A series of interferograms showing the grease film behavior in the contact area corresponding to the rolling condition and the sliding condition are shown in Figs. 7a and 8a, respectively. The reference line is marked by the broken line.

In the case of rolling microoscillation, as shown in Fig. 7a, there is no relative displacement between the glass disk and the entrapped grease. The shape of the entrapped grease remains almost unchanged while moving in the Hertzian contact area. The displacements of the disk, the ball, and the entrapped grease in one cycle are plotted in Fig. 7b. It can be seen that the displacement of the entrapped grease is the same as that of the glass disk during one cycle. It can be deduced that the relative motion does not occur between the glass disk and the entrapped grease under the rolling microoscillation.

However, in the case of sliding microoscillation, the reference line moves faster than the entrapped grease, and the shape of the entrapped grease has no obvious change while moving in the Hertzian contact area, as shown in Fig. 8a. The displacements of the disk, the entrapped grease, and the ball in one cycle are plotted in Fig. 8b. It can be seen that the displacement of the entrapped grease is smaller than that of the disk. Therefore, it can be deduced that the relative motions occur at the two interfaces of the grease/disk and the grease/ball at the same time under the sliding microoscillation.

How does the relative motion occur in the contact area by using grease under the sliding microoscillation? In the contact area, the viscosity of the grease increases with the contact pressure. The variation of the grease viscosity can be expressed by:

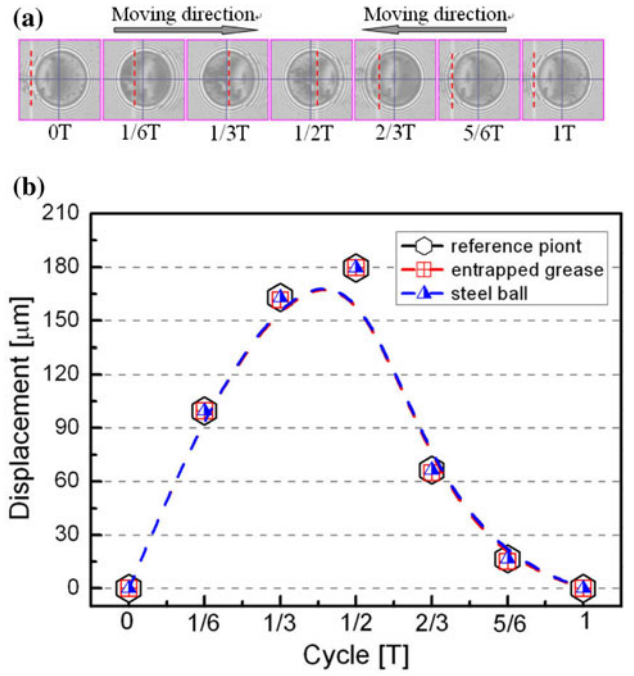

Fig. 7 The movement of the entrapped grease under the rolling microoscillation (load is 14 N, rolling amplitude is 0.176 mm): **a** Interferograms in one cycle. **b** The displacement variation of the disk surface, ball surface, and entrapped grease in the contact region

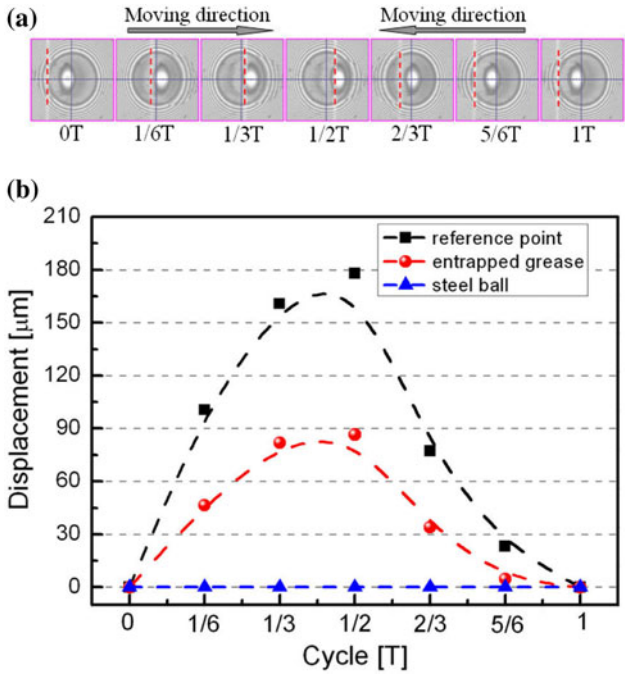

Fig. 8 The movement of the entrapped grease under the sliding microoscillation (load is 14 N, rolling amplitude is 0.176 mm): **a** Interferograms in one cycle. **b** The displacement variation of the disk surface, ball surface, and entrapped grease in the contact region

$$\eta = \eta_0 e^{ap} \tag{2}$$

where η is the viscosity of the grease at a given pressure, η_0 is the viscosity of the grease at the atmospheric pressure, e is the constant of 2.718, α is the pressure/viscosity coefficient, and p is the applied pressure. The Herschel–Bulkley flow model was used by Kauzlarich and Greenwood [24] to describe the inlet rheology of grease:

$$\tau = \tau_{cg} + \eta\gamma^n \tag{3}$$

$$\tau_{cg} = \tau_0 e^{ap} \tag{4}$$

where τ is the shear stress, τ_{cg} is the critical yield shear stress that the grease can sustain, that is, the grease will flow when the shear stress exceeds the τ_{cg} in the contact area, γ is the shear rate, and n is a constant (<1), τ_0 is the yield shear stress of the grease at the atmospheric pressure.

In order to obtain the contact pressure in the entrapped region, the finite element method was used to calculate the pressure in the entrapped grease. The method was based on the following assumptions:

1. The entrapped grease in the contact area was considered as a rigid body.
2. The shape of the entrapped grease abode by the cosine function, and the entrapped grease was just at the center of the contact area.
3. The contact stress that can deform the disk and ball in the contact area is close to the pressure in the entrapped grease.

In this way, the shape of the entrapped grease can be expressed by:

$$h = h_0 \cos\theta = h_0\left(\cos\frac{\pi x}{2r_0}\right) \tag{5}$$

where h is the entrapped grease film thickness, h_0 is the maximum entrapped grease film thickness ($h_0 = 200$ nm), x is the distance from one point to the center point of the contact area, and r_0 is the radius of the entrapped grease ($r_0 = 48$ μm).

Figure 9 shows the schematic diagram of finite element model. The pressure distribution in the contact area is shown in Fig. 10. It can be seen that the pressure increased rapidly in the entrapped grease region as compared with other regions in the Hertzian contact area. The mean pressure of the entrapped grease region is about 0.85 GPa in the sliding tests. As shown in Fig. 11, the critical yield shear stress of the grease at atmospheric pressure is 244 Pa. According to Eq. 4, the critical yield shear stress of the entrapped grease is 32.3 GPa. If the entrapped grease flows under the sliding microoscillation condition, the coefficient of friction exceeds 115. In fact, the coefficient of friction in point contact by using grease is about 0.1. It at least implies that the grease in the contact area can be considered as a

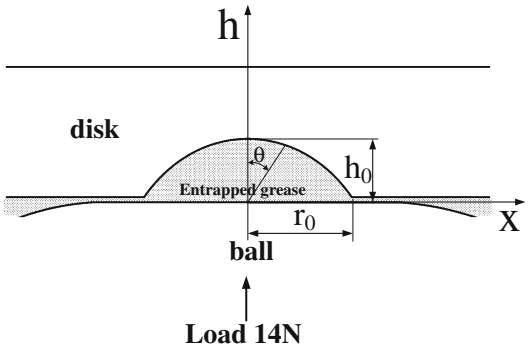

Fig. 9 The schematic diagram of the finite element model

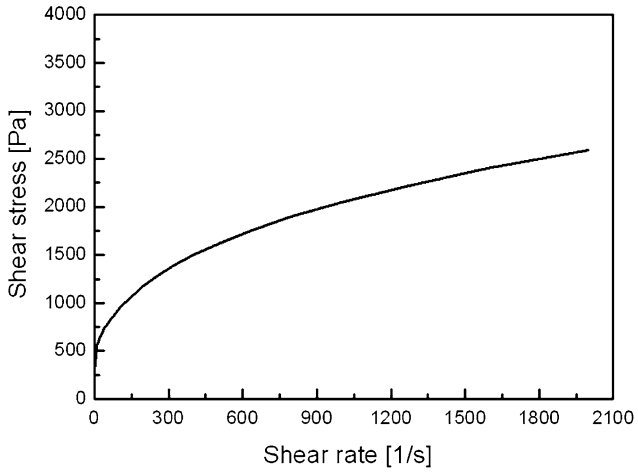

Fig. 11 Rheological curve of the grease

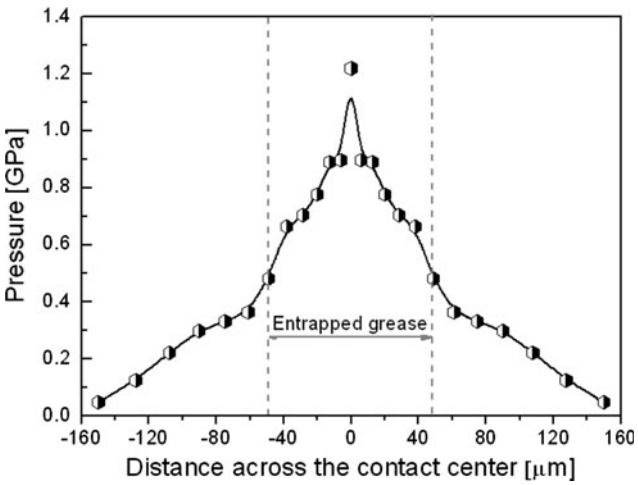

Fig. 10 The distribution of the pressure in the contact region

solid material in a glassy state [25, 26]. In tests, with the disk sliding, the entrapped grease can hardly flow due to the large critical yield shear stress. Only when the shear stress exceeds the critical yield shear stress of the grease/disk interface or the grease/ball interface, the relative motion can occur.

4.2 Formation and Motion of Grease Film in Central Contact Area

In this part, the behaviors of the newly formed grease film will be discussed. The process of the formation and motion of the grease film in rolling condition is shown in Fig. 12. The film thickness profiles correspond to the given positions (section plane) on the interferograms. The processes of the formation and the motion of the grease film in sliding condition are shown in Fig. 13. As can be seen from Figs. 12a and 13a, once the grease film formed in the inlet region, the film thickness profile is almost unchanged during moving in the contact area [8]. The film thickness is affected considerably by the fluctuation of the entrainment

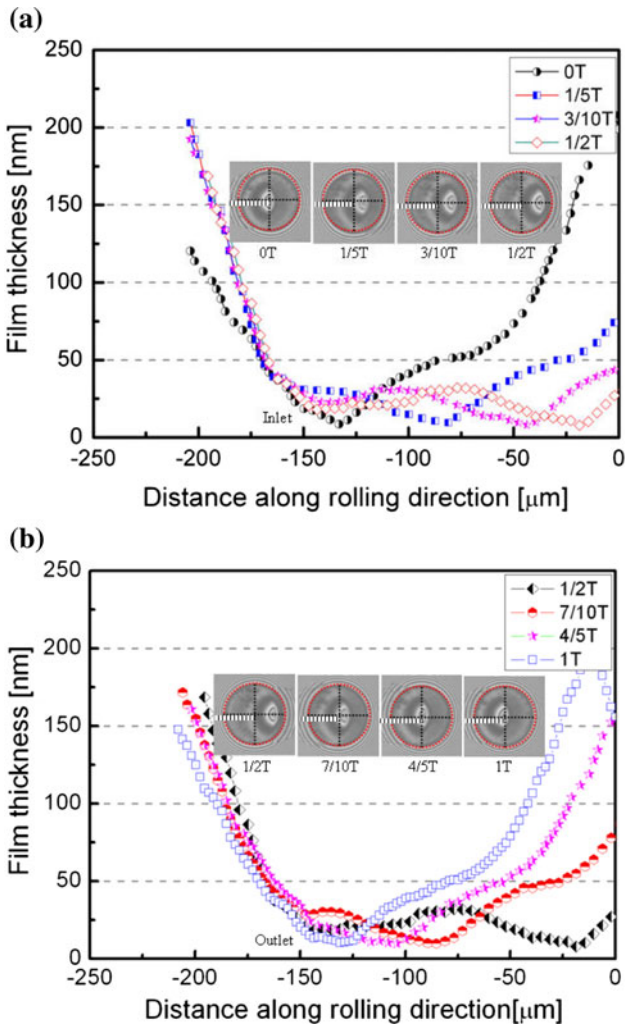

Fig. 12 Process of the grease film formation/disrepair in the rolling microoscillation: **a** Formation of the grease film. **b** Disrepair of the formed grease film

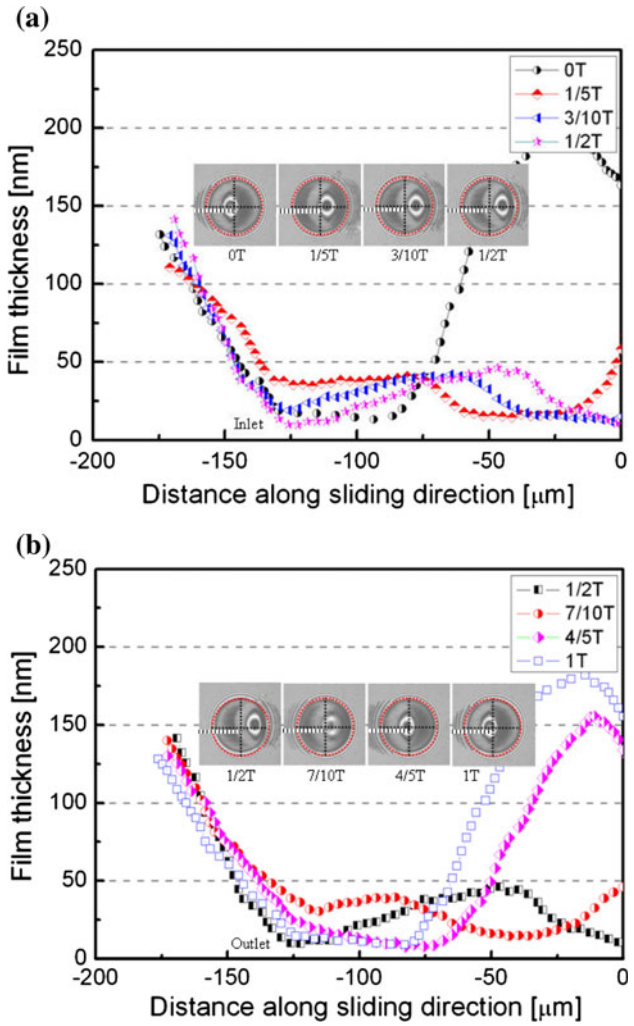

Fig. 13 Process of the grease film formation/disrepair in the sliding microoscillation: **a** Formation of the grease film. **b** Disrepair of the formed grease film

velocity under microoscillation [27, 28]. After reversal, as shown in Figs. 12b and 13b, the formed grease film moves to the outlet, and the film thickness profile of the formed grease film remains largely unchanged before the formed grease film enter the outlet zone.

The maximum width of the newly formed grease film coincides with the amplitude of the microoscillation under the rolling condition. However, the maximum width of the newly formed grease film is smaller than the amplitude of the microoscillation under the sliding condition, and it is due to the occurrence of relative motion between the formed grease film and the working surfaces [9, 19].

4.3 Variation of the Grease Film Thickness Under Microoscillation

It is always assumed that sufficient grease is present in the inlet to form the grease film. In fact, the film formation

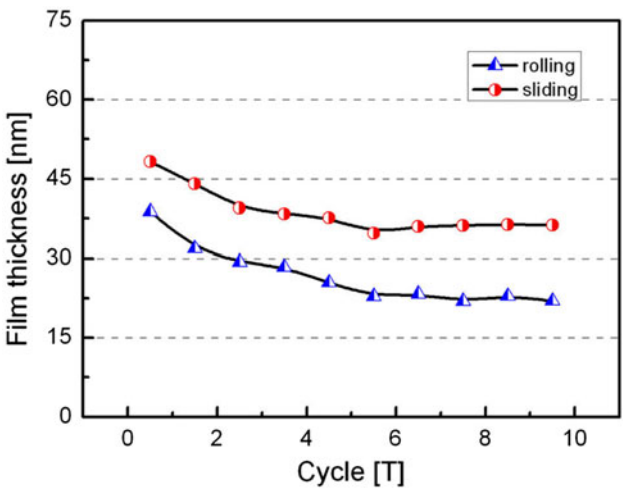

Fig. 14 The variations of the formed maximum film thickness with the repetition of microoscillations

characteristic is also influenced by the lubricant supply to the contact area. The rheological properties of grease are complex and dependent on both the shear rate and the duration of shearing [6]. At a low shear rate, the grease behaves as a plastic solid and does not flow until a critical yield stress has been reached. Thus, once the grease has been pushed to either side of the rolling/sliding track by the passage of the ball, it would not be a spontaneous flow back to replenish the inlet immediately. Therefore, the inlet of the contact area is only partially filled and the film thickness is reduced from the fully flooded value. Then, starvation occurs rapidly near the inlet region and the grease film thickness drops. It can be seen from Fig. 14, the newly formed maximum grease film thickness decreases during the repeated microoscillation. Obviously, the supply of the grease lubricant to the contact area plays an important role in determining the grease film thickness. In fact, under microoscillation, it is not easy to supply the contact area with the grease and finally the contact area is in a lubricant starved condition. Thereby, with the repeated microoscillation, the number of the grease lubricant molecules entering into the contact area decreases and the grease film thickness drops gradually. Once little grease lubricant is present in the contact area, lubricating failure happens. Consequently, the friction should increase and the surface could be damaged easily.

5 Conclusion

The behaviors of the grease film in the contact area in a microoscillation process have been investigated. Experimental results indicate that the grease film is formed in the inlet region, and its thickness profile remains almost unchanged in one cycle during motion in the contact area.

A crescent-shaped film has been observed in the contact area. In the case of the rolling microoscillation condition, the crescent-shaped grease film and the entrapped grease film are carried by the two moving surfaces at the same velocity. However, in the case of the sliding microoscillation condition, relative motions occur both at the two interfaces of the grease/ball and the grease/disk. Under the same microoscillation amplitude, the maximum width of the crescent-shaped film without the relative motion is larger than that with the relative motion. During repetition of microoscillations, the crescent-shaped grease film thickness drops gradually, and ultimately the lubrication failure would occur.

Acknowledgments The work is financially supported by the Natural Science Foundation of China (50721004) and 973 Project (2006CB705403 and 2007CB607604). The authors would like to thank NSK Ltd. for providing the high precision steel balls.

References

1. Cann, P.M.: Starved grease lubrication of rolling contacts. Tribol. Trans. **42**, 867–873 (1999)
2. Cann, P.M., Lubrecht, A.A.: An analysis of the mechanisms of grease lubrication in rolling element bearings. Lubr. Sci. **11**, 227–245 (1999)
3. Wedeven, L.D., Evans, D., Cameron, A.: Optical analysis of ball bearing starvation. Trans. ASME J. Lubr. Tech. **93**, 349–363 (1971)
4. Palacios, J.M., Cameron, A., Arizmendi, L.: Film thickness of grease in rolling contacts. Tribol. Trans. **24**, 474–478 (1981)
5. Cann, P.M.: Grease lubrication of rolling element bearings-role of the grease thickener. Lubr. Sci. **19**, 183–196 (2007)
6. Cann, P.M., Williamson, B.P., Coy, R.C., Spikes, H.A.: The behaviour of greases in elastohydrodynamic contacts. J. Phys. D Appl. Phys. **25**, A124–A132 (1992)
7. Glovnea, R.P., Spikes, H.A.: Behavior of EHD films during reversal of entrainment in cyclically accelerate/deceleration motion. Tribol. Trans. **45**, 177–184 (2002)
8. Sugimura, J., Jones, W.R., Spikes, H.A.: EHD film thickness in non-steady state contacts. ASME J. Tribol. **120**, 442–452 (1998)
9. Glovnea, R.P., Spikes, H.A.: Elastohydrodynamic film formation at the start-up of the motion. Proc. Inst. Mech. Eng. J: J. Eng. Tribol. **215**, 125–138 (2001)
10. Kalin, M., Joze, V.: The tribological performance of DLC coatings under oil-lubricated fretting conditions. Tribol. Int. **39**, 1060–1067 (2006)
11. Kaneta, M., Takeshima, T., Togami, S., Nishikawa, H.: Stribeck curve in reciprocating seals. Proc. 18th Int. Conf. On Fluid Sealing, pp. 333–347 (2005)
12. Ikeuchi, K., Fujita, S., Ohashi, M.: Analysis of fluid film formation between contacting compliant solids. Tribol. Int. **31**, 613–618 (1998)
13. McColl, I.R., Waterhouse, R.B., Harris, S.J., Tsujikawa, M.: Lubricated fretting wear of a high-strength eutectoid steel rope wire. Wear **185**, 203–212 (1996)
14. Zhou, Z.R., Kapsa, P.h., Vincent, L.: Grease lubrication in fretting. ASME J. Tribol. **120**, 737–743 (1998)
15. Glovnea, R.P., Spikes, H.A.: The influence of lubricant on film collapse rate in high pressure thin film behaviour during sudden halting of motion. Tribol. Trans. **43**, 731–739 (2000)
16. Luo, J.B., Wen, S.Z., Huang, P.: Thin film lubrication. Part I. Study on the transition between EHL and thin film lubrication using a relative optical interference intensity technique. Wear **194**, 107–115 (1996)
17. Luo, J.B., Shen, M.W., Wen, S.Z.: Tribological properties of nanoliquid film under an external electric field. J. Appl. Phys. **96**, 6733–6738 (2004)
18. Li, G., Zhang, C.H., Luo, J.B.: Film-forming characteristics of grease in point contact under swaying motions. Tribol. Lett. **35**, 57–65 (2009)
19. Guo, F., Wong, P.L., Geng, M., Kaneta, M.: Occurrence of wall slip in elastohydrodynamic lubrication contacts. Tribol. Lett. **34**, 103–111 (2009)
20. Wong, P.L., Lingard, S., Cameron, A.: The high-pressure impact microviscometer. STLE Tribol. Trans. **35**, 500–508 (1992)
21. Kaneta, M., Ozaki, S., Nishikawa, H., Guo, F.: Effects of impact loads on point contact elastohydrodynamic lubrication films. Proc. IMechE J: J. Eng. Tribol. **221**, 271–278 (2007)
22. Dowson, D., Jones, D.A.: Lubricant entrapment between approaching elastic solids. Nature **214**, 947–948 (1967)
23. Kaneta, M., Nishikawa, H., Kameishi, K.: Observation of wall slip in elastohydrodynamic lubrication. ASME J. Tribol. **112**, 447–452 (1990)
24. Kauzlarich, J.J., Greenwood, J.A.: Elastohydrodynamic lubrication with Herschel-Bulkley model greases. Tribol. Trans. **15**, 269–277 (1972)
25. Smith, F.W.: Lubricant behaviour in concentrated contact systems-some rheological problems. ASLE Trans. **3**, 18–25 (1960)
26. Jacobson, B.O.: An experimental determination of the solidification velocity for mineral oils. ASLE Trans. **17**, 290–294 (1974)
27. Ren, N., Zhu, D., Wen, S.Z.: Experimental method for quantitative analysis of transient EHL. Tribol. Int. **24**, 225–230 (1991)
28. Glovnea, R.P., Diaconescu, E.N., Flamand, L.: EHD film thickness under transient speed conditions. Acta Tribol. **13**, 31–36 (1995)